sustainability

MDPI

Article

Optimizing Hempcrete Properties Through Thermal Treatment of Hemp Hurds for Enhanced Sustainability in Green Building

Veronica D'Eusanio [1,2,*], Mirco Rivi [1,2], Daniele Malferrari [1,3] and Andrea Marchetti [1,2,3]

[1] Department of Chemical and Geological Sciences, University of Modena and Reggio Emilia, 41125 Modena, Italy; 270475@studenti.unimore.it (M.R.); daniele.malferrari@unimore.it (D.M.); andrea.marchetti@unimore.it (A.M.)
[2] National Interuniversity Consortium of Materials Science and Technology (INSTM), 50121 Firenze, Italy
[3] Interdepartmental Research Center BIOGEST-SITEIA, University of Modena and Reggio Emilia, 42124 Reggio Emilia, Italy
* Correspondence: veronica.deusanio@unimore.it

Abstract: This study examines the effects of the thermal pre-treatment of hemp hurds on the physical, mechanical, and thermal properties of hempcrete, evaluating its potential as a sustainable building material. Hemp hurds were pre-treated at various temperatures (120–280 °C) and characterized by proximate analysis, CHNS elemental analysis, and thermogravimetric analysis (TGA). The resulting hempcrete samples were analyzed for density, water absorption, compressive strength, and thermal conductivity. Three different hempcrete formulations, with varying lime:hemp proportions, were analyzed. The findings indicate that higher pre-treatment temperatures lead to reduced density and water absorption across all formulations. Formulations containing a higher hemp hurd content had lower densities but higher water absorption values. Compressive strength increased consistently with the pre-treatment temperature, suggesting that higher temperatures enhance matrix bonding and structural rigidity, and with the lime content. However, thermal conductivity also rose with pre-treatment, with only the composition containing the highest hemp hurd content maintaining the optimal insulation threshold (0.1 W/mK). This suggests a trade-off between compressive strength and insulation performance, influenced by the balance of hemp hurd and lime content. These findings underscore the potential of thermal pre-treatment to tailor hempcrete properties, promoting its application as a durable, moisture-resistant material for sustainable building, though the optimization of hurd–lime ratios remains essential.

Keywords: hempcrete; hemp hurds; sustainability; green building; TGA; compressive strength; thermal conductivity

Citation: D'Eusanio, V.; Rivi, M.; Malferrari, D.; Marchetti, A. Optimizing Hempcrete Properties Through Thermal Treatment of Hemp Hurds for Enhanced Sustainability in Green Building. *Sustainability* **2024**, *16*, 10404. https://doi.org/10.3390/su162310404

Academic Editor: Graziano Salvalai

Received: 8 November 2024
Revised: 24 November 2024
Accepted: 27 November 2024
Published: 27 November 2024

1. Introduction

Hemp, an annual botanical species of the *Cannabaceae* family, is gaining recognition for its high versatility as a crop [1–4]. As the focus on sustainable and multifunctional agricultural production grows, hemp cultivation is also expanding the investigation of its many potential uses and applications in various industries. Numerous semi-finished products that serve as the primary raw material for a wide range of end-use products have been produced as a result of modern hemp production. Products like clothes, ropes, and carpets are made from long hemp fibers [5,6]. In the manufacturing of paper, geotextiles, and composite materials, short fibers provide more ecologically favorable options [7,8]. Hemp hurd, the woody core of the stalk, finds application in the construction industry, where it is used to create thermal and sound insulation panels, known as hempcrete [9–11]. These materials are mixed with water and hydrated lime to obtain a lightweight composite building material that has appreciable benefits for sustainable construction.

Lightweight building materials, generally having a density range of 300 to 1800 kg/m^3, are known for their reduced environmental impact due to features such as increased ther-

mal insulation, sound absorption, and better ease of transportation and handling [12–16]. The reduced density results in decreased dead loads on constructions, which allows for more efficient architectural designs with less heavy structural reinforcements. This decreases not only the demand for raw materials, but also improves transportation efficiency, hence reducing fuel and energy use in building logistics. Furthermore, the superior thermal insulating properties of hempcrete contribute to energy efficiency in buildings by keeping indoor temperatures stable, therefore minimizing the need for heating and cooling systems, in good agreement with sustainable construction requirements and goals of carbon reduction [17,18]. Hempcrete also contributes to carbon sequestration in two ways [19–22]. First, when growing, the hemp plant absorbs large amounts of carbon dioxide from the atmosphere through the process of photosynthesis. Second, during the production of hempcrete, the hemp shives are combined with lime and water, thereby starting a carbonation reaction. The calcium hydroxide ($Ca(OH)_2$) contained in the lime binder reacts with atmospheric CO_2 to form calcium carbonate ($CaCO_3$), which is a more stable compound, durable [23], and the effective binder in the mature mixture. This carbonation process does not stop after the hempcrete has set as the construction stage, but continues over a very long period, thus absorbing CO_2 and sequestering carbon to enhance the environmental sustainability of the material.

The major drawbacks of hempcrete are its very long drying time and low mechanical strength [24–26], which are directly related to the physical and chemical properties of hemp hurds, mainly comprising cellulose, hemicellulose, and lignin. Cellulose, accounting for approximately 45–52% of hemp hurds [27,28], is a linear polysaccharide formed from hundreds to thousands of β(1→4)-linked glucose units [29]. With a strong presence of free hydroxyl groups, cellulose is strongly hydrophilic and thus easily forms hydrogen bonds with water molecules in its vicinity. Hemicellulose, an amorphous polysaccharide, accounting for about 20–25% of hemp hurds [27,28], exhibits lower thermal stability than cellulose [30]. Hemicellulose has a lower degree of polymerization with a variety of sugars, including pentoses and hexoses, providing higher water absorption compared to cellulose. The synergistic presence of high cellulose and hemicellulose content is responsible for the hygroscopic nature of hemp hurds. The third major constituent, lignin, makes up around 15–25% of the hemp hurds [27,28]. Lignin is a phenolic polymer that structurally supports the material, thereby providing strength and resistance to microbial degradation [31]. Although lignin has lower hydrophilicity compared to cellulose and hemicellulose, its concentration is insufficient to counteract the high-water-retention capacities of the other components. Thus, high moisture retention in hemp hurds significantly impacts the drying and curing processes of hempcrete, which therefore extends construction times, increases costs, and poses challenges for project management, especially in a cold and humid climate. This high moisture retention slows the carbonation of the lime binder, a process essential for developing a dense, structurally sound final product [32,33]. Similarly, excess water in the mixture inhibits the diffusion of CO_2, which is necessary for efficient carbonation and impacts hempcrete's capacity to develop mechanical properties and durability. Additionally, excessive moisture weakens the bond between hemp and the lime binder, lowering the material's overall structural stability. This inherent porosity of hempcrete further accentuates these problems by weakening the bonding between the hemp hurds and the binder. If aeration is inadequate, high humidity can result in biodeterioration, freeze–thaw action, and salt crystallization, all leading to material deterioration and decreasing hempcrete's lifespan.

To enhance hemp hurd's performance in hempcrete mixtures and lessen its strong hygroscopic nature, a range of pre-treatments can be applied. Surface modification of the fibers by grafting hydrophobic compounds or short polymers is a widely used approach to decrease hydrophilicity, thus improving the compatibility of natural fibers for biocomposite applications [10,27,34–36]. Although these chemical approaches are efficient, they can be costly and environmentally unsafe due to the chemicals involved. Thermal treatments have therefore great potential to be more cost-effective and environmentally friendly alternatives. The application of low-energy thermal treatments, such as streaming

or mild pyrolysis, eliminates the need for chemical approaches and decreases the water affinity of lignocellulosic biomass by modifying the hydrophilic nature of cellulose and hemicellulose [37,38]. The potential to improve biomass stability is the most evident advantage of such treatments. It is well known that thermal treatment successfully suppresses microbial activity, halting fermentation and other phenomena that could otherwise result in the emission of toxic gasses, including methane [39]. While low-temperature thermal treatments require an input of energy, there is considerable scope for improving the overall energy efficiency through the recovery and reutilization of heat generated during treatment. This extra thermal energy, arising during steaming or pyrolysis, can be further utilized for the preheating of incoming biomass or as an energy source for additional processes in order to minimize the overall demand for energy [39]. Although thermal treatment potentially increases the moisture resistance of hempcrete, there remains a lack of research into its detailed effects on the mechanical and physical properties of hempcrete made from preheated hemp hurds. In this study, thermal pre-treatment was performed on hemp hurds at temperatures ranging from 120 to 280 °C in an inert atmosphere. Such treatment is known to degrade hemicellulose preferentially, which starts degrading in this temperature range, resulting in mass loss and structural changes that may reduce water uptake. In contrast, cellulose is relatively thermally stable, maintaining its structure mainly below 250 °C, with no significant devolatilization. The use of low temperatures, below 300 °C, is also important to obtain a high yield of materials. High temperatures would lead to a significant degradation of cellulose and lignin, lowering the material yield and possibly affecting the mechanical properties of the treated hurds.

Proximate analysis and thermogravimetric analysis (TGA) were carried out to determine the properties of treated hemp hurd samples. This research aims at investigating how thermal pre-treatment affects the key properties of hempcrete, which includes compressive strength, density, thermal conductivity, and water absorption. In this study, these effects are investigated, and an attempt is made to bridge the gap in the literature and deliver insights into the optimization of hempcrete for wider construction applications.

2. Materials and Methods

2.1. Hemp Hurd Samples

Hemp hurd samples were obtained from Centro Qualità Tessile S.r.l. (Carpi, Modena, Italy), a research laboratory specialized in the analysis of textile fibers, including hemp fibers. The batch of hemp hurds was of Italian origin and was previously air-dried. Nine samples were thermally pre-treated in an inert atmosphere for 6 h at the following temperatures: 120, 160, 200, 240, and 280 °C. One sample was left untreated. Thermal pre-treatment has a marked effect on the color of the hurd, which gradually becomes darker. As an example, Figure S1 shows the air-dried (AD) hemp hurds (left) and those pre-treated at 240 °C (right).

2.2. Lime

Hydrated lime from Litokol S.p.A. (Rubiera, Italy) was used to prepare the hempcrete samples, and its physical and chemical properties are presented in Table S1.

2.3. Hempcrete Specimen Preparation

Hempcrete specimens were prepared by mixing hemp hurds with hydrated lime and enough water to achieve good workability and easy compaction within the molds. The samples were molded into dimensions of 4 cm × 4 cm × 8 cm.

2.4. Formulation and Design of Hempcrete Mixtures

Three different formulations with varying hemp–lime–water ratios were evaluated. These formulations were selected based on several literature studies [25,40–42], and the specific compositions are presented in Table 1.

Table 1. Mixing proportions of the hempcrete specimens.

	Proportions (vol%)		
Formulation	**Hemp Hurd**	**Lime**	**Water**
A	80	12	8
B	75	15	10
C	65	20	15

The samples were labeled by combining the formulation type (A, B, and C) with the pre-treatment temperature of the hemp hurds. For example, sample A120 is composed of a type A formulation with hemp hurds pre-treated at 120 °C; the CAD sample consists of a type C formulation with air-dried hemp hurds. All formulations were prepared according to percentage composition by volume, since hemp experiences a weight reduction during thermal treatment.

2.5. Proximate Analysis, CHNS Elemental Analysis, and Determination of Bulk Density and Water Absorption

Moisture, ash, protein, and protein contents were determined following the methods recommended by the Association of Official Analytical Chemists [43]. Moisture content was determined by drying the samples at 105 °C to a constant weight. The ash content was determined using a laboratory furnace at 550 °C, and the temperature gradually increased. The Dumas method was used to determine the nitrogen content, which was converted to protein content by multiplying it by a factor of 6.25. The Soxhlet method was used to determine the residual fat fraction using petroleum ether (boiling point range: 40–60 °C) as the extractant solvent. Each measurement was performed in triplicate, and the results were averaged. CHNS elemental analysis was conducted using a CHNS Analyzer Flash2000 instrument (Thermo Scientific, Waltham, MA, USA). The bulk density of the hempcrete samples was determined by pouring them into a graduated glass cylinder. The bulk density was calculated by dividing the mass by the volume in by the cylinder. Five replicates were performed for each measurement and the results were averaged.

Water absorption tests were conducted on plant-based raw materials according to the ASTM C 127 [44] and ASTM C 128 standards [45]. Approximately 1 g of material was immersed in 15 mL of water for 24 h. The material was then filtered, surface-dried, and weighed. The result is expressed as a percentage of water absorption, calculated as the difference between the mass of the dry material and the mass after water absorption. Five replicates were performed for each measurement and the results were averaged.

2.6. Thermogravimetric Analysis (TGA)

Thermogravimetric analysis was conducted on the hemp hurd samples using a Seiko SSC 5200 thermal analyzer (Seiko Instruments Inc., Chiba, Japan) under inert atmosphere conditions. The heating protocol employed a gradient of 10 °C min^{-1} over a temperature range of 25–1000 °C, with ultrapure helium purging at a flow rate of 100 µL min^{-1}.

2.7. SEM Analysis

The field emission scanning electron microscope (SEM) instrument (Nova NanoSEM 450, FEI, Hillsboro, OR, USA) was used to evaluate the microscopic morphology of the hemp hurd and hempcrete samples. A heating system, consisting of a heating stage, a voltmeter with a platinum–rhodium thermocouple, and a heating control unit, was used. The temperature was increased at the rate of 4 °C/min.

2.8. Compressive Strength of the Hempcrete Specimens

Compressive strength tests were performed after 14 and 28 days of curing using a Tecnotest compression test machine (Tecnotest, Modena, Italy).

2.9. Density of the Hempcrete Specimens

To calculate the density of the specimens, their masses were recorded after 28 days of curing. These masses were then divided by the volume of the specimen (256 cm^3).

2.10. Water Absorption of the Hempcrete Specimens

Water absorption was determined following the ASTM C642-21 procedure [46]. Specimens were immersed in deionized water for 24 h. After immersion, the specimens were removed from the water, and any excess water on the surfaces was carefully wiped away using a clean, dry cloth. Each specimen was weighted before and after immersion. Water absorption was calculated based on the weight difference between the water-immersed specimens and the dry specimens, expressed as a percentage of the initial dry weight.

2.11. Thermal Conductivity of the Hempcrete Specimens

Thermal conductivity was performed on the specimens after 28 days of curing. It was measured using a KD2 Pro thermal property analyzer (Decagon Inc., Pullman, WA, USA). This portable device fully complies with ASTM D5334-08 [47] and is used to measure the thermal properties of materials using the transient-line heat-source method. The KD2 Pro is equipped with various interchangeable sensors that measure thermal conductivity, thermal diffusivity, and specific heat. The measurement involved heating the probe for a specific period and monitoring the temperature during heating and cooling. To obtain more accurate values, the influence of ambient temperature on the samples must be minimized; therefore, measurements should be conducted under consistent thermal environmental conditions. The measurement range of the KD2 Pro for thermal conductivity was between 0.02 and 2.00 W/(mK).

2.12. Data Analysis

Data analyses were conducted using Matlab R2023a (The Mathworks Inc., Natick, MA, USA).

3. Results and Discussion

3.1. Proximate Analysis of the Hemp Hurd Samples

The data in Table 2 present a detailed analysis of hemp hurd samples subjected to thermal treatments at various temperatures ranging from 120 to 280 °C. The results include moisture, protein, lipids, and ash, as well as the results of the CHNS analysis, including C, H, N, S, and O contents. Some physical properties, i.e., bulk density and water absorption, were also included.

The moisture content of hemp hurd samples showed a consistent and significant decline as the treatment temperature increased, starting from 9.96 wt% in the air-dried sample (AD) and dropping to 0.581 wt% by 280 °C. A sharp drop between 120 and 200 °C can be attributed to the evaporation of both free water (which is easily released) and bound water (which is more tightly associated with the material's structure), and near-complete moisture removal was reached at 280 °C. The minimized residual moisture decreases susceptibility to mold and fungal growth, contributing to the material's long-term durability in damp environments.

The protein content showed an initial decrease from 2.25 wt% in the AD sample to 1.53 wt% after treatment at 120 °C, followed by a gradual increase to 2.63 wt% after treatment at 280 °C. This initial drop is likely due to protein denaturation or partial degradation, a process common at lower temperature values, which disrupts the protein structure. As the primary constituents break down and volatile organic compounds (VOCs) and moisture are lost, the proportion of protein in the solid residue appears to increase. Since proteins normally only degrade at temperatures higher than those examined in this work, this change represents the change in the relative concentration brought on by the breakdown of non-protein components.

Table 2. Proximate analysis, CHNS elemental analysis, and some physical properties of the hemp hurd samples. Data followed by different letters within the same row indicate statistically differences ($p < 0.05$).

Sample	AD	120	160	200	240	280
Moisture (wt%)	9.96 ± 0.23^{a}	5.80 ± 0.14^{b}	3.61 ± 0.33^{c}	1.32 ± 0.19^{d}	0.758 ± 0.072^{e}	0.581 ± 0.080^{e}
Protein (wt%)	2.25 ± 0.09^{a}	1.53 ± 0.08^{b}	1.60 ± 0.08^{bc}	1.90 ± 0.15^{c}	2.22 ± 0.13^{a}	2.63 ± 0.14^{d}
Lipids (wt%)	<0.1	<0.1	<0.1	<0.1	<0.1	<0.1
Ash (wt%)	1.10 ± 0.01^{a}	1.16 ± 0.05^{a}	1.50 ± 0.05^{b}	1.92 ± 0.06^{c}	2.80 ± 0.15^{d}	3.72 ± 0.12^{e}
C (wt%)	46.2 ± 1.9^{a}	47.3 ± 1.0^{a}	47.9 ± 0.2^{a}	48.0 ± 0.1^{a}	50.9 ± 0.2^{b}	52.4 ± 0.4^{b}
H (wt%)	5.82 ± 0.11^{ab}	5.68 ± 0.13^{ab}	5.85 ± 0.07^{b}	5.84 ± 0.14^{ab}	5.65 ± 0.15^{ab}	5.53 ± 0.05^{a}
N (wt%)	0.35 ± 0.03^{ac}	0.24 ± 0.04^{b}	0.26 ± 0.02^{a}	0.32 ± 0.05^{abc}	0.35 ± 0.04^{abc}	0.42 ± 0.03^{c}
S (wt%)	<0.1	<0.1	<0.1	<0.1	<0.1	<0.1
O# (wt%)	46.5 ± 2.0^{a}	45.6 ± 0.8^{a}	44.5 ± 0.2^{a}	43.9 ± 0.2^{a}	40.3 ± 0.5^{b}	38.0 ± 0.6^{b}
Bulk density (g/mL)	0.117 ± 0.002^{a}	0.114 ± 0.003^{ab}	0.108 ± 0.004^{bc}	0.106 ± 0.001^{cd}	0.103 ± 0.001^{cde}	0.098 ± 0.001^{e}
Water absorption (%)	263 ± 2^{a}	262 ± 3^{ab}	255 ± 4^{b}	245 ± 2^{c}	232 ± 2^{d}	191 ± 3^{e}

= by difference.

As was to be expected for lignocellulosic materials, which typically contain very little fat, the lipid content was extremely low, below 0.1 wt%, at all temperatures.

The ash content increased steadily with the temperature, rising from 1.10 wt% in the AD sample to 3.72 wt% after treatment at 280 °C. This increase results from the thermal degradation of the organic components, which decompose and are lost as volatiles, as well as the moisture removal, leaving inorganic residues concentrated in the residual material. Application in hempcrete may benefit from a higher ash content, potentially enhancing fire resistance and thermal stability, as the inorganic fraction is less combustible.

The carbon content in the hemp hurd samples increased significantly from 46.2 wt% in the AD sample to 52.4 wt% after treatment at 280 °C, indicating progressive carbonization. This is because organic components like cellulose and hemicellulose break down, releasing volatile compounds containing oxygen, hydrogen, and nitrogen while leaving behind a carbon-rich residue. Since fewer stable components are removed during the thermal degradation process, this carbon concentration increases the material's thermal stability and carbon density. The hydrogen content remained relatively constant, ranging from 5.5 to 5.8 wt%, and tended to decrease slightly as the pre-treatment temperature increased. This slight decrease is probably due to the removal of water during heat treatment and the slow loss of volatile hydrogen-containing molecules, such as hydroxyl groups. As the temperature rose, the nitrogen content increased somewhat, shifting from 0.24 to 0.42 wt%. This pattern suggests that, as other components, primarily carbohydrates, are eliminated as a result of heat breakdown, nitrogen becomes relatively more concentrated. Proteins and other nitrogenous molecules are either not greatly broken down or are maintained in a stable form at these temperatures, as seen by the comparatively low nitrogen levels. As the pre-treatment temperature increased, the oxygen concentration decreased from 46.5 to 38.0 wt%. The loss of oxygen-rich VOCs, water, and carbon dioxide, released during the thermal degradation of hemicellulose and cellulose, is responsible for this trend. The drop in oxygen offers further assistance to the carbonization process of the specimen, which makes the material gradually consist of more stable carbon components.

Following treatment at 280 °C, the bulk density dropped from 0.117 g/mL in the AD sample to 0.098 g/mL, suggesting a consistent mass loss as the temperature rose. This decrease is caused by the loss of moisture and organic components subject to thermal degradation. A lower aggregate weight of building applications, such as hempcrete, has significant benefits. It not only leads to the overall reduction in the building material itself, resulting in improved handling, reduced costs, and greenhouse gas emissions associated with transportation, but also leads to a reduction in the structural load in building applica-

tions. These aspects have the main effect of improving the sustainability and efficiency of the entire building process.

Water absorption decreased from 263% in the AD sample to 191% after treatment at 280 °C, primarily due to the degradation of hemicellulose, a highly hydrophilic component. In addition, lignin content increases with temperature, and, due to its greater hydrophobicity, also contributes to the reduction in water absorption and an improvement in moisture resistance. Reduced water absorption makes hemp more suitable for construction applications, as it leads to a reduction in the possibility of damage, such as swelling, structural deterioration, and microbiological growth, which threaten its longevity and durability.

3.2. Thermogravimetric Analysis (TGA) of the Hemp Hurds

Thermogravimetric analysis is a widely used analytical technique to assess the thermal stability and composition of materials. In this study, TGA was used to investigate the effect of heat treatment on the composition of hemp hurds, particularly on the alteration in the content of lignocellulosic components.

The thermogravimetric (TG) and its first derivative (DTG) curves of the AD hemp hurds, shown in Figure 1, provide a basis for understanding the composition of the material before any thermal alteration. A summary of the TGA results is provided in Table 3, which shows all the thermally activated processes that occurred in the temperature range examined.

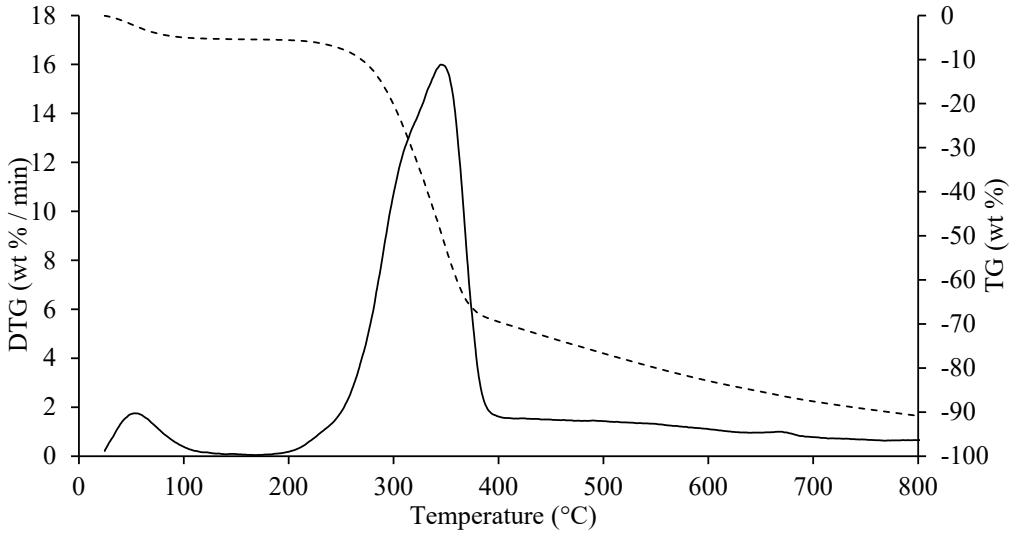

Figure 1. TG (dashed) and DTG (solid) curves of the air-dried hemp hurds.

The TG/DTG profile of the sample follows the typical trend observed in lignocellulosic materials [48,49]. The thermogram can be divided into five regions, each corresponding to specific thermal events that occurred within the biomass matrix. Region I, which covers the temperature range up to ~120 °C, represents the initial drying phase, primarily involving moisture removal and the evaporation of VOCs, which contribute to the matrix's characteristic aroma (Δm wt% = 5.22). Other thermally activated processes, such as protein denaturation via unfolding [50,51], occur in this region without significant mass loss. Region II, which covers the temperature range from ~120 to ~210 °C, is related to the release of bound water, typically associated with inorganic components, like mineral salts, along with the complete removal of semi-volatile compounds present in the initial matrix or generated during heating (Δm wt% = 0.480). Around 160 °C, structural water begins to be released due to condensation reactions of hydroxyl groups in simple non-cellulosic carbohydrates [52]. The formation and removal of reaction waters travers the entire thermogram, up to and including region IV. Near the upper temperature limit of region II (~180 °C), free amino acids begin to undergo thermal degradation processes [53], while proteins persist up to ~210 °C. Thus, the processes occurring in this region suggest that the chemical structure of the biomass begins to destabilize, partly depolymerize,

and plasticize. Region III, subtended in the temperature range from ~210 to ~415 °C, represents the main pyrolysis window where the structural decay of proteins (~240 °C), hemicellulose (~300 °C) [54,55], and cellulose (~370 °C) [50,55,56] are observed. The mass loss in this region is approximately Δm wt% = 64.9. Region IV beings at ~415 °C and extends up to ~700 °C. In this thermal range, the gradual mass decrease (Δm wt% = 16.9) is mainly due to the slow pyrolysis of the lignin fraction [57,58], which is associated with the vitrification and volatilization of carbon microparticles. A minor thermal event near 660 °C can be attributed to the decomposition of carbonaceous material, likely biochar derived from the hemicellulosic fraction [59,60], although lignin components may also contribute to its formation [61]. The literature studies also associate this thermal event with the decomposition of carbonates with the release of CO_2. In region V, above ~700 °C, the last residues of biomass degradation can be observed. This is the typical pyrolysis window involving the thermal decomposition of low volatile matter (Δm wt% = 3.75), such as carbon fragments C20–C40, in presence of mineral ashes.

Table 3. Results of the TGA analysis of the air-dried hemp hurds, comprising the description of the thermally activated process.

Region	To (°C)	Tm (°C)	Tc (°C)	Δm wt%	Thermally Activated Processes
I	24.6	53.2	120.5	5.22	Removal of moisture and VOCs.
II	120.5	-	210.3	0.480	Removal of bound water, NH_3 from protein denaturation, low-boiling VOCs, and loss of CO and CO_2.
III	210.3	345.6	415.3	64.9	Protein degradation, removal of reaction and constitutional water, low-boiling VOCs, decarboxylation of acids with CO_2 loss, degradation of polysaccharides, plasticization, and pseudo-vitrification of the sample.
IV	415.3	-	700.2	16.9	Removal of reaction water, and weak reactions related to slow volatilization of CO_2 and carbon residues.
V	700.2	-	814.8	3.75	Volatilization of carbon residues (C20–C40 fragments)

To = onset temperature (beginning of thermal step processes). Tm = maximum temperature for the largest mass loss rate. Tc = conclusion temperature (end of thermal step processes).

The TG and DTG curves of the thermally pre-treated hemp hurds are shown in Figure 2.

In region III (210–415 °C), where the primary degradation of hemicellulose and cellulose occurs, some changes in the DTG curve profile can be observed. At lower pre-treatment temperatures (160 and 200 °C), hemicellulose degradation appears as a shoulder around 300 °C. This shoulder progressively decreases in intensity, disappearing completely at pre-treatment temperatures of 240 and 280 °C. This indicates that higher pre-treatment temperatures induce the substantial thermal alteration or partial decomposition of hemicellulose, consistent with previous studies [49,56,61]. Consequently, the onset of the main degradation signal in region III shifts to higher temperatures in the samples pre-treated at 240 and 280 °C. This observation suggests increased thermal stability within the hemicellulose–cellulose fraction due to structural changes induced by thermal pre-treatment. These structural changes probably result from cross-linking, dehydration, and condensation reactions in the hemicellulose and cellulose. Furthermore, the less evident degradation peak is partly due to partial hemicellulose decomposition and mass loss during pre-treatment, which reduces the fraction available for degradation. Importantly, cellulose maintains its structural integrity even after pre-treatment up to 280 °C, consistent with the literature reports that cellulose degradation typically starts above 300 °C. Although the complete decomposition of cellulose is not achieved within the pre-treatment temperature range, gradual reductions in the cellulose degradation signal intensity suggest that the material undergoes preliminary thermal modification without a full breakdown, requiring higher temperatures for complete degradation. In the higher temperature range (above 400 °C), a

significant mass loss is observed in the samples pre-treated at 200 °C or above related to thermal degradation or lignin. The increase in the fraction of mass lost in this region confirms that increasing pre-treatment temperatures leads to the loss and partial degradation of the most thermo-unstable fractions, hemicellulose and cellulose, with the consequent enrichment of the more thermoresistant lignin content.

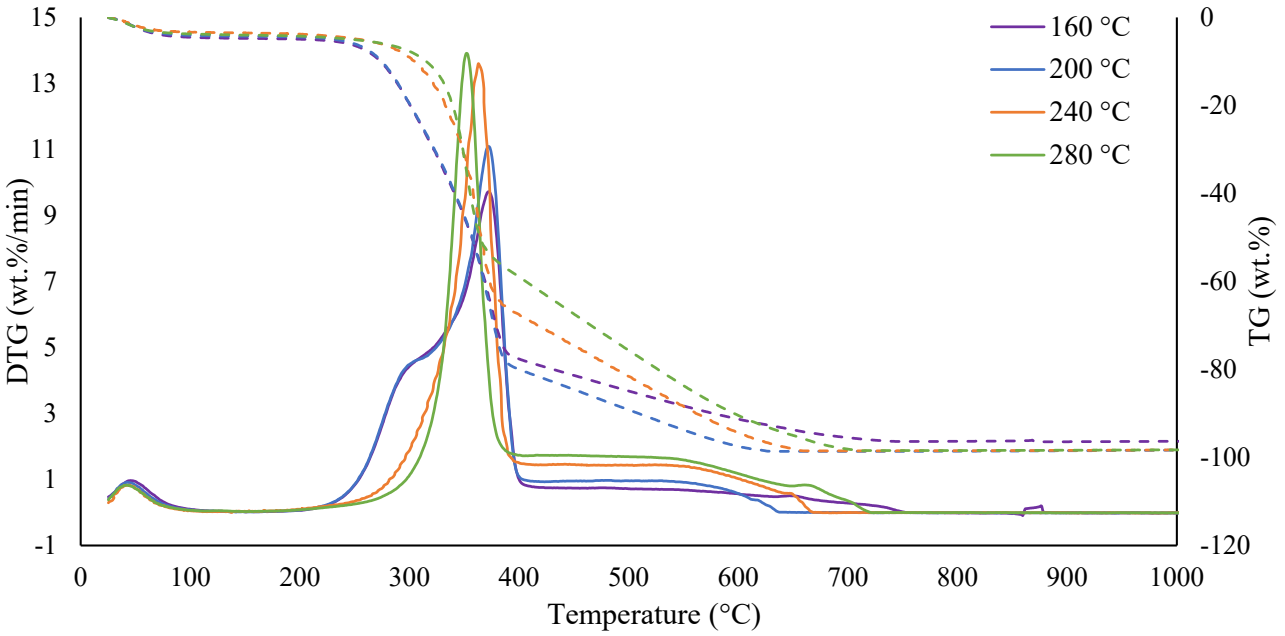

Figure 2. TG (dashed) and DTG (solid) curves of the thermally treated hemp hurd samples.

3.3. SEM Analysis

In this study, SEM analysis was performed to closely investigate the microstructure and morphology of AD hemp hurds, explore their interaction with lime in the hempcrete composite, and assess any morphological changes following thermal treatment. This information is valuable for gaining a deeper understanding of the mechanical and physical properties of hempcrete.

SEM images of the AD hemp hurds are shown in Figure 3.

SEM analysis shows a complex and heterogeneous microstructure in the AD hemp hurds. Both the internal and external surfaces have alternating regions of compact and dense fibrous material and more filamentous areas, which are characterized by numerous cavities, grooves, and significant porosity. This porosity greatly enhances the internal surface area of the material. The fibrous regions likely consist of tightly bound cellulose, hemicellulose, and lignin, which contribute to the structural integrity of the plant material. Conversely, the porous structure facilitates capillary absorption, enabling the lime slurry to penetrate deeply into the hemp hurds during mixing. This process allows carbonation to occur directly within the pores of the hurds, resulting in the stiffening of the lignocellulosic structures and an improvement in the mechanical properties of the final composite. Furthermore, the interaction between the lime solution and the free hydroxyl and carboxyl groups found in the biopolymers (cellulose, hemicellulose, and lignin) of the hurds promotes a strong bond at the interface between the organic (hurd) and inorganic (lime) components of the composite.

To investigate this interaction, a small fragment of hempcrete with the "B" formulation (BAD sample) was micro-crushed and analyzed after 28 days of curing (Figure 4).

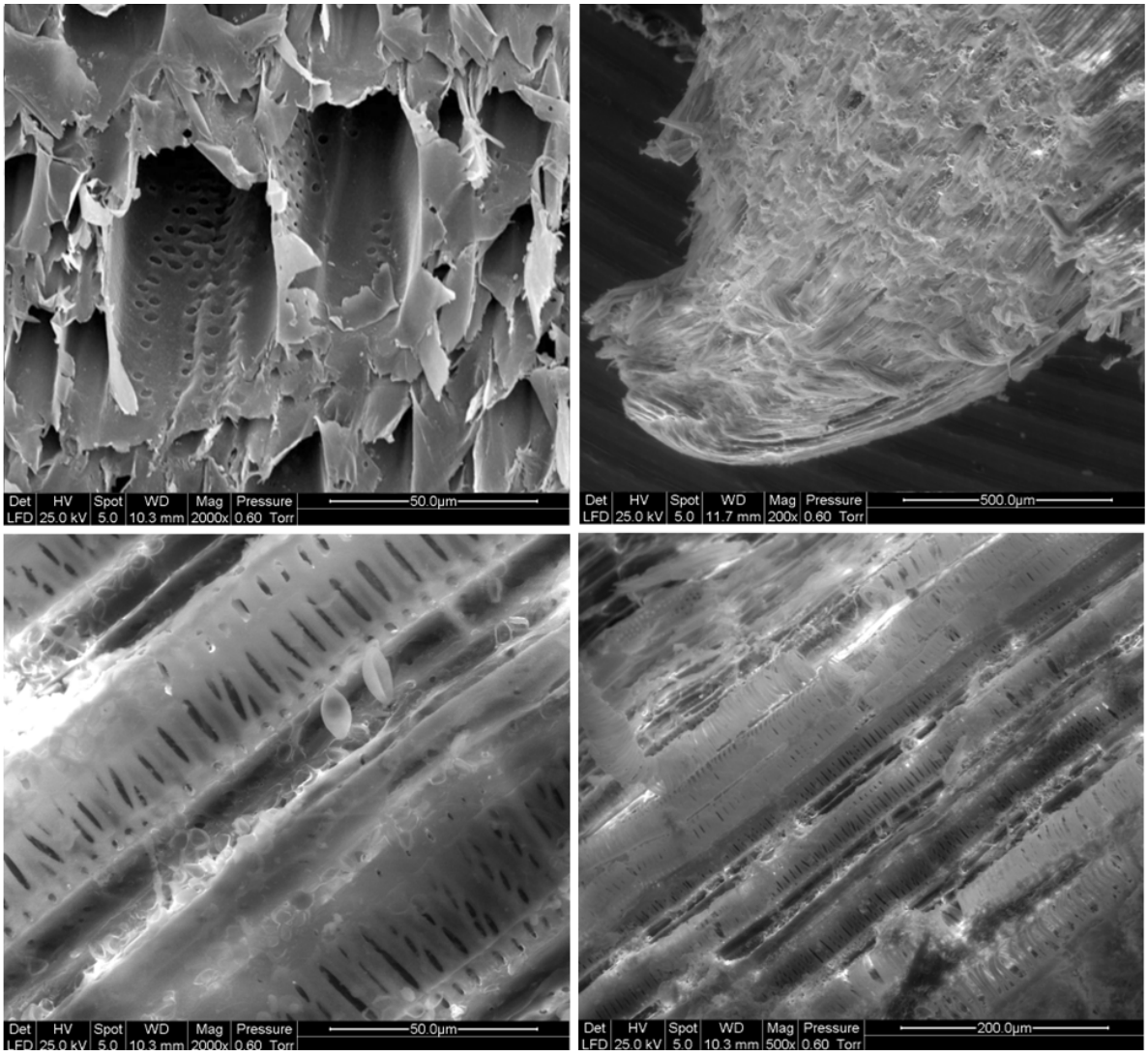

Figure 3. Internal (**up**) and external (**down**) surfaces of an air-dried hemp hurd sample.

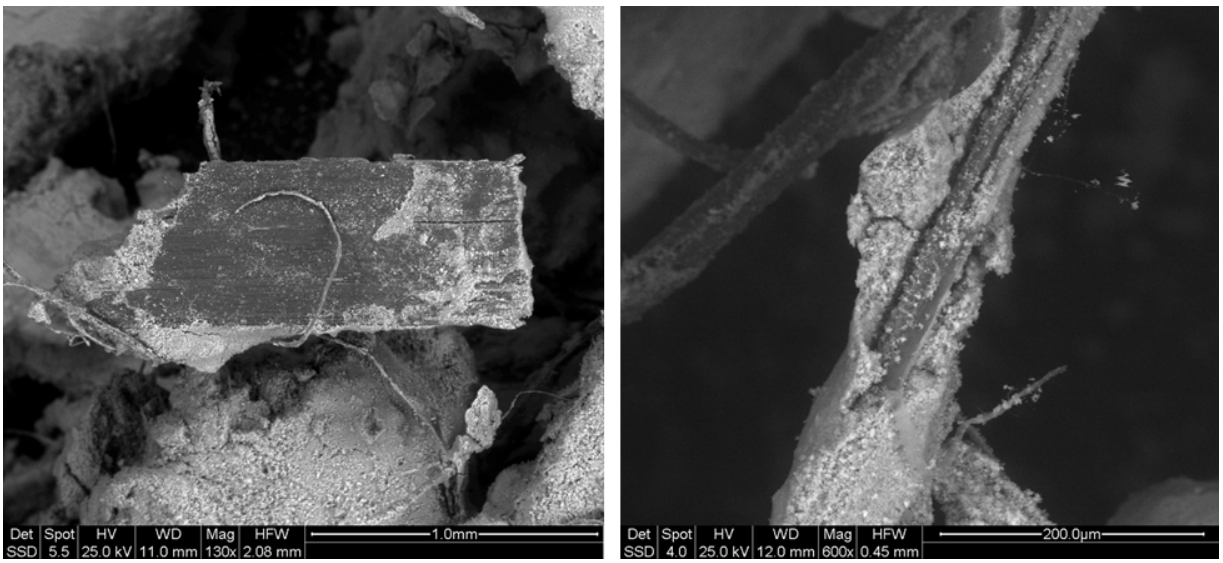

Figure 4. Fragment of hemp hurd extracted from BAD hempcrete specimen: front (**left**) vs. lateral (**right**) view.

The images from this analysis show the microstructural features and interaction zones between the lime binder and the hurds. In particular, a hemp microfiber about 25 µm thick is covered by a lime layer of a fairly consistent thickness, about 40 µm. Lime was observed to infiltrate the pores and grooves of the hurds, initiating carbonation within the internal voids of the hurds' structure.

Further SEM analysis was performed on a hemp hurd sample heated at different temperatures during analysis. These SEM images are shown in Figure 5.

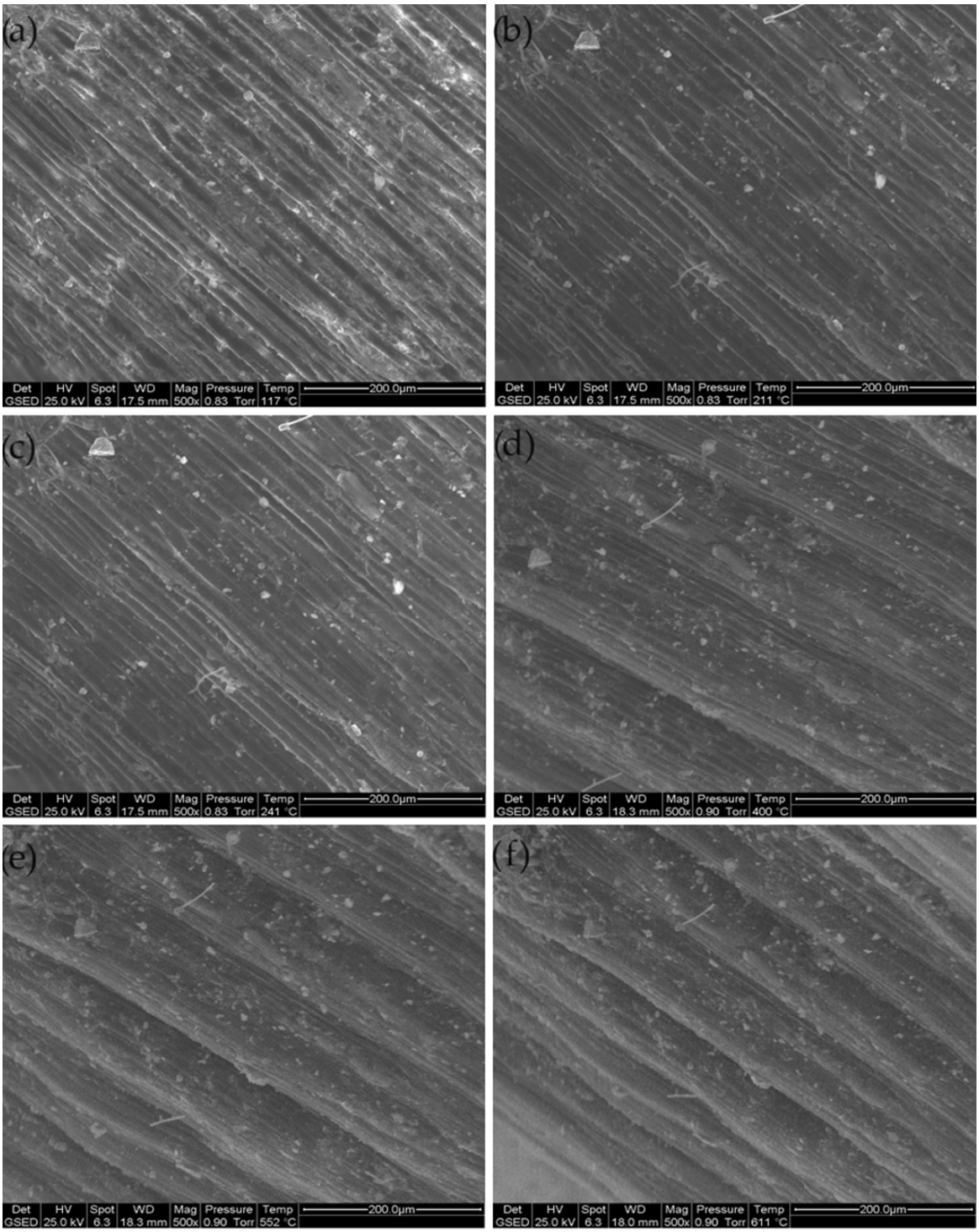

Figure 5. EDS analysis of a hemp hurd sample treated at 117 °C (**a**), 211 °C (**b**), 241 °C (**c**), 400 °C (**d**), 552 °C (**e**), and 611 °C (**f**).

The pre-treatment did not drastically alter the overall structure of the lignocellulosic matrix. The porous structure remained largely intact, and the observed crumpling and deformation of the longitudinal fibers indicated the gradual removal of simple volatile molecules (e.g., H_2O, CO, and CO_2) during the pyrolysis process. While these processes resulted in minor mass loss, they did not significantly impact the basic morphology of the shives, suggesting that the thermal pre-treatment preserved the structural integrity of the material while inducing some fiber contraction and pore expansion.

3.4. Hempcrete Properties: Density, Water Absorption, Compressive Strength, and Thermal Conductivity

Table 4 summarizes the density, water absorption, compressive strength, and thermal conductivity of hempcrete samples (A, B, and C). Each formulation displays unique trends influenced by the hemp hurd content and pre-treatment temperatures.

Table 4. Density (kg/m^3), water absorption (%), compressive strength (kPa), and thermal conductivity (W/mK) of the hempcrete samples. Data followed by different letters within the same column indicate statistically significant differences ($p < 0.05$).

	Density (14 d) (kg/m^3)	Density (28 d) (kg/m^3)	Water Absorption (%)	Compressive Strength (kPa)	Thermal Conductivity (W/mK)
AAD	$397 \pm 10^{\text{ah}}$	$309 \pm 11^{\text{a}}$	$121.1 \pm 13.3^{\text{a}}$	$318 \pm 13^{\text{a}}$	$0.047 \pm 0.007^{\text{a}}$
A120	$401 \pm 19^{\text{abh}}$	$312 \pm 14^{\text{a}}$	$118.3 \pm 3.7^{\text{a}}$	$331 \pm 19^{\text{a}}$	$0.057 \pm 0.009^{\text{ab}}$
A160	$400 \pm 11^{\text{ach}}$	$298 \pm 9^{\text{a}}$	$116.1 \pm 17.0^{\text{ab}}$	$325 \pm 28^{\text{a}}$	$0.063 \pm 0.004^{\text{abc}}$
A200	$365 \pm 12^{\text{ad}}$	$281 \pm 11^{\text{ab}}$	$90.3 \pm 9.5^{\text{bc}}$	$383 \pm 16^{\text{ab}}$	$0.072 \pm 0.002^{\text{bcd}}$
A240	$328 \pm 16^{\text{de}}$	$240 \pm 15^{\text{bc}}$	$72.9 \pm 8.8^{\text{cd}}$	$466 \pm 22^{\text{cd}}$	$0.080 \pm 0.001^{\text{cde}}$
A280	$308 \pm 8^{\text{e}}$	$225 \pm 20^{\text{c}}$	$63.9 \pm 7.0^{\text{d}}$	$515 \pm 31^{\text{cd}}$	$0.081 \pm 0.002^{\text{cde}}$
BAD	$452 \pm 17^{\text{bfh}}$	$382 \pm 17^{\text{di}}$	$114.5 \pm 7.4^{\text{ab}}$	$334 \pm 22^{\text{a}}$	$0.088 \pm 0.007^{\text{de}}$
B120	$467 \pm 22^{\text{fgh}}$	$400 \pm 5^{\text{dhi}}$	$114.2 \pm 5.0^{\text{ab}}$	$452 \pm 42^{\text{bc}}$	$0.089 \pm 0.011^{\text{de}}$
B160	$432 \pm 32^{\text{h}}$	$379 \pm 13^{\text{di}}$	$104.2 \pm 9.4^{\text{abce}}$	$375 \pm 32^{\text{a}}$	$0.096 \pm 0.007^{\text{e}}$
B200	$421 \pm 21^{\text{h}}$	$362 \pm 16^{\text{de}}$	$80.9 \pm 6.3^{\text{cde}}$	$498 \pm 32^{\text{cd}}$	$0.118 \pm 0.007^{\text{f}}$
B240	$358 \pm 15^{\text{ae}}$	$321 \pm 18^{\text{ae}}$	$67.6 \pm 5.7^{\text{cf}}$	$511 \pm 11^{\text{cd}}$	$0.134 \pm 0.006^{\text{fg}}$
B280	$328 \pm 8^{\text{de}}$	$298 \pm 22^{\text{a}}$	$58.7 \pm 7.9^{\text{d}}$	$540 \pm 26^{\text{d}}$	$0.142 \pm 0.008^{\text{gh}}$
CAD	$506 \pm 14^{\text{gi}}$	$469 \pm 10^{\text{f}}$	$104.8 \pm 6.8^{\text{ab}}$	$512 \pm 18^{\text{cd}}$	$0.121 \pm 0.005^{\text{f}}$
C120	$497 \pm 14^{\text{fi}}$	$451 \pm 26^{\text{fg}}$	$103.5 \pm 5.5^{\text{ab}}$	$513 \pm 19^{\text{cd}}$	$0.128 \pm 0.007^{\text{fg}}$
C160	$491 \pm 9^{\text{fi}}$	$443 \pm 16^{\text{fh}}$	$95.5 \pm 8.8^{\text{abc}}$	$532 \pm 18^{\text{d}}$	$0.137 \pm 0.002^{\text{fgh}}$
C200	$485 \pm 14^{\text{fi}}$	$438 \pm 11^{\text{fh}}$	$76.7 \pm 10.0^{\text{bcd}}$	$677 \pm 12^{\text{e}}$	$0.149 \pm 0.007^{\text{gi}}$
C240	$474 \pm 18^{\text{fi}}$	$432 \pm 17^{\text{fh}}$	$62.1 \pm 7.2^{\text{df}}$	$777 \pm 22^{\text{f}}$	$0.156 \pm 0.005^{\text{hi}}$
C280	$449 \pm 19^{\text{cfh}}$	$418 \pm 17^{\text{gi}}$	$52.4 \pm 6.3^{\text{df}}$	$829 \pm 26^{\text{f}}$	$0.166 \pm 0.003^{\text{i}}$

The density values for all examined formulations decreased consistently with longer curing times and higher hurd pre-treatment temperatures. Notably, except for samples CAD and C120, all formulations achieved density values within the ideal range for low-bearing, non-structural materials (250–450 kg/m^3), which are designed for applications requiring thermal insulation and sound absorption. Higher pre-treatment temperatures across all formulations lead to lower densities due to hurd bulk density reduction and increased hydrophobicity. Since formulation A contained the highest proportion of hemp hurds, it exhibited the lowest densities, while formulation C, with the highest lime content, had the highest values. Formulation A showed the greatest density reduction with increasing pre-treatment temperature after 28 days of curing, from 309 kg/m^3 (AAD) to 225 kg/m^3

(A280). From 14 to 28 days, the average decrease in density across all formulation A samples was approximately 24%. Formulation C showed a less pronounced density reduction with increasing pre-treatment temperature after 28 days of curing, from 469 kg/m^3 (CAD) to 418 kg/m^3 (C280). The average density decrease from 14 to 28 days of curing was 9%. The slower reduction in density during curing observed in formulation C samples was likely due to the higher water content associated with lime. In fact, lime's ability to chemically bind water during hydration results in a slower release of water during curing, contributing to a more gradual density reduction [33]. Formulation B showed an intermediate density reduction, reflecting its moderate hurd and lime composition.

The water absorption decreased significantly with increasing pre-treatment temperature, which can be attributed to the higher hydrophobicity and to the structural changes in the hemp hurds. Formulation A had the greatest water absorption capacity, which reduced from 121.1% (AAD) to 63.9% (A280) with increasing pre-treatment temperature, resulting in a 47% decrease. This trend indicates a strong correlation between thermal treatment and reduced water affinity, which aligns with the increased hydrophobicity of the hemp hurds due to the loss of hydroxyl groups from hemicellulose, as previously pointed out. The increase in lime content leads to less water absorption, since moisture retention is mainly influenced by the hemp hurd content. Formulations B and C similarly presented decreased water absorption with increasing the pre-treatment temperature, but to lesser extent due to the different hurd content values. Across all formulations, a marked decline was observed between 160 and 200 °C of pre-treatment temperatures, signifying a shift toward hydrophobic behavior in this range.

Compressive strength increased across all formulations with increasing hurd pre-treatment temperatures, indicating that the thermal modification of the hemp hurds enhanced the material's mechanical properties. This improvement can likely be attributed to the thermal decomposition of organic components in the hurds, making them more brittle. This results in the mixture being more easily compacted during the test specimen roll-out, resulting in denser, stiffer, void-free composites. Additionally, higher pre-treatment temperatures may accelerate the carbonation reaction within the lime binder, as less water is retained within the mixture, further promoting matrix consolidation and the faster development of compressive strength, producing higher values after 28 days of curing. Formulation A's strength rises from 318 kPa (AAD) to 515 kPa (A280), a 62% improvement. Formulation C shows the highest compressive strength, reaching 829 kPa for the C280 sample, indicating greater structural integrity due to its denser, lime-rich matrix. The values of formulation B samples fall between those of formulations A and C.

Thermal conductivity increases with higher pre-treatment temperatures across all formulations, reflecting a denser material structure with an enhanced heat conduction capacity. This increase can also be attributed to the higher carbon content in the thermally treated hemp hurds, indicating a greater presence of carbonaceous materials, which are generally more thermally conductive. The AAD sample has the lowest thermal conductivity value of 0.047 W/mK, which increases to 0.081 W/mK after treatment at 280 °C, showing an overall 72% increase. This low thermal conductivity reflects the high organic content and air pockets within the structure, which enhance the insulation properties. Formulation B shows a higher thermal conductivity value of 0.088 W/mK for the BAD sample, compared to the corresponding AAD sample. Thermal conductivity increases to 0.142 W/mK after the pre-treatment of the hurds at 280 °C, marking a 61% increase. This formulation has more lime content than formulation A, leading to a denser structure and higher conductivity at each temperature. Formulation C consistently shows the highest thermal conductivity, starting at 0.121 W/mK (CAD) and peaking at 0.166 W/mK after pre-treatment at 280 °C, representing a 37% increase. A building material with thermal conductivity below 0.1 W/mK is generally considered a good insulator. Despite the increase in conductivity following the heat pre-treatment of the hemp hurds, formulation A remains within this desirable threshold, maintaining good insulation properties. However, the same does not apply to formulations B and C, where the higher lime content causes the conductivity to exceed the 0.1 W/mK

limit. This suggests a potential limitation to the use of heat pre-treatment in applications requiring optimal insulation. To achieve a material with a good insulation performance, it is beneficial to maintain a higher proportion of hemp hurds and limit the lime content, though this may compromise the compressive strength.

4. Conclusions

This study demonstrates that the pre-treatment temperature of hemp hurds significantly influences the physical and mechanical properties of hempcrete, with implications for its use as a sustainable building material. Increasing pre-treatment temperatures of the hurds led to notable reductions in density and water absorption across all hempcrete formulations, which is advantageous for applications requiring lightweight insulating materials with enhanced moisture resistance. The marked decrease in water absorption, particularly at temperatures above 200 °C, reflects the structural modifications and increased hydrophobicity of the hemp hurds, likely due to the thermal degradation of hemicellulose and cellulose. Compressive strength showed a consistent increase with higher pre-treatment temperatures, suggesting that elevated temperatures improve the rigidity and bonding within the hemp–lime matrix. This enhancement is attributed to the removal of hydroxyl groups and the partial degradation of organic components, which together produce a denser, more mechanically robust structure. However, thermal conductivity also increased with higher pre-treatment temperatures. Despite the increased conductivity following the heat pre-treatment of hemp hurds, formulation A remains within this desirable threshold, maintaining effective insulation properties. The same does not apply to formulations B and C, where the higher lime content causes the conductivity to exceed the 0.1 W/mK limit. This suggests a potential limitation to heat pre-treatment in applications requiring an optimal insulation performance. To achieve effective insulation, a higher proportion of hemp hurds with limited lime content may be advantageous, though this may compromise the compressive strength. Overall, the findings highlight that the thermal pre-treatment of hemp hurds can be strategically used to tailor hempcrete's properties for specific construction applications. Pre-treated hemp hurds not only enhance the material's structural and thermal performance, but also support long-term sustainability in construction by improving durability and reducing the need for additional moisture-resistant additives.

This preliminary study lays the groundwork for numerous future investigations, which could address a variety of critical aspects. Future research should focus on optimizing the thermal pre-treatment parameters to maximize the performance and evaluate the long-term durability of hempcrete under variable environmental conditions. Additionally, upcoming studies should examine the energy consumption associated with the thermal pre-treatment of hemp shives, offering a thorough evaluation of the overall sustainability of the resulting hempcrete.

Supplementary Materials: The following supporting information can be downloaded at: https://www.mdpi.com/article/10.3390/su162310404/s1, Figure S1: Air-dried hemp hurds (left) and pre-treated at 240 °C (right); Table S1: Physical and chemical properties of the hydrated lime used in this study.

Author Contributions: Conceptualization, V.D. and M.R.; methodology, V.D. and D.M.; software, V.D. and A.M.; validation, V.D., A.M. and D.M.; formal analysis, V.D.; investigation, V.D. and M.R.; resources, V.D. and A.M.; data curation, V.D. and M.R.; writing—original draft preparation, V.D.; writing—review and editing, D.M. and M.R.; visualization, V.D. and A.M.; supervision, A.M.; project administration, A.M. and D.M.; funding acquisition, V.D. and A.M. All authors have read and agreed to the published version of the manuscript.

Funding: This research received no external funding.

Institutional Review Board Statement: Not applicable.

Informed Consent Statement: Not applicable.

Data Availability Statement: Data are contained within the article.

Acknowledgments: It is a pleasure to gratefully thank Centro Qualità Tessile S.r.l. (Carpi (MO), Italy) for providing us with the hemp hurds used in this study.

Conflicts of Interest: The authors declare no conflicts of interest.

References

1. Crini, G.; Lichtfouse, E.; Chanet, G.; Morin-Crini, N. Traditional and New Applications of Hemp. In *Sustainable Agriculture Reviews 42: Hemp Production and Applications*; Crini, G., Lichtfouse, E., Eds.; Springer: Cham, Switzerland, 2020; pp. 37–87. ISBN 978-3-030-41384-2.
2. Zhao, X.; Wei, X.; Guo, Y.; Qiu, C.; Long, S.; Wang, Y.; Qiu, H. Industrial Hemp—An Old but Versatile Bast Fiber Crop. *J. Nat. Fibers* **2022**, *19*, 6269–6282. [CrossRef]
3. Nath, M.K. Benefits of Cultivating Industrial Hemp (*Cannabis sativa* ssp. Sativa)—A Versatile Plant for a Sustainable Future. *Chem. Proc.* **2022**, *10*, 14. [CrossRef]
4. Rehman, M.; Fahad, S.; Du, G.; Cheng, X.; Yang, Y.; Tang, K.; Liu, L.; Liu, F.-H.; Deng, G. Evaluation of Hemp (*Cannabis sativa* L.) as an Industrial Crop: A Review. *Environ. Sci. Pollut. Res.* **2021**, *28*, 52832–52843. [CrossRef]
5. Muzyczek, M. 4—The Use of Flax and Hemp for Textile Applications. In *Handbook of Natural Fibres*, 2nd ed.; Kozłowski, R.M., Mackiewicz-Talarczyk, M., Eds.; The Textile Institute Book Series; Woodhead Publishing: Cambridgeshire, UK, 2020; pp. 147–167. ISBN 978-0-12-818782-1.
6. Vandepitte, K.; Vasile, S.; Vermeire, S.; Vanderhoeven, M.; Van der Borght, W.; Latré, J.; De Raeve, A.; Troch, V. Hemp (*Cannabis sativa* L.) for High-Value Textile Applications: The Effective Long Fiber Yield and Quality of Different Hemp Varieties, Processed Using Industrial Flax Equipment. *Ind. Crops Prod.* **2020**, *158*, 112969. [CrossRef]
7. Ranalli, P.; Venturi, G. Hemp as a Raw Material for Industrial Applications. *Euphytica* **2004**, *140*, 1–6. [CrossRef]
8. Crini, G.; Lichtfouse, E.; Chanet, G.; Morin-Crini, N. Applications of Hemp in Textiles, Paper Industry, Insulation and Building Materials, Horticulture, Animal Nutrition, Food and Beverages, Nutraceuticals, Cosmetics and Hygiene, Medicine, Agrochemistry, Energy Production and Environment: A Review. *Environ. Chem. Lett.* **2020**, *18*, 1451–1476. [CrossRef]
9. Benfratello, S.; Capitano, C.; Peri, G.; Rizzo, G.; Scaccianoce, G.; Sorrentino, G. Thermal and Structural Properties of a Hemp–Lime Biocomposite. *Constr. Build. Mater.* **2013**, *48*, 745–754. [CrossRef]
10. Qiu, R.; Ren, X.; Fifield, L.S.; Simmons, K.L.; Li, K. Hemp-Fiber-Reinforced Unsaturated Polyester Composites: Optimization of Processing and Improvement of Interfacial Adhesion. *J. Appl. Polym. Sci.* **2011**, *121*, 862–868. [CrossRef]
11. Shahzad, A. Hemp Fiber and Its Composites—A Review. *J. Compos. Mater.* **2012**, *46*, 973–986. [CrossRef]
12. Haque, M.N.; Al-Khaiat, H.; Kayali, O. Strength and Durability of Lightweight Concrete. *Cem. Concr. Compos.* **2004**, *26*, 307–314. [CrossRef]
13. Thienel, K.-C.; Haller, T.; Beuntner, N. Lightweight Concrete—From Basics to Innovations. *Materials* **2020**, *13*, 1120. [CrossRef]
14. D'Eusanio, V.; Bertacchini, L.; Marchetti, A.; Mariani, M.; Pastorelli, S.; Silvestri, M.; Tassi, L. Rosaceae Nut-Shells as Sustainable Aggregate for Potential Use in Non-Structural Lightweight Concrete. *Waste* **2023**, *1*, 549–568. [CrossRef]
15. D'Eusanio, V.; Anderlini, B.; Marchetti, A.; Pastorelli, S.; Roncaglia, F.; Ughetti, A. Exploring the Potential of Peach (*Prunus persica* L.) Nut-Shells as a Sustainable Alternative to Traditional Aggregates in Lightweight Concrete. *Multidiscip. J. Eng. Sci.* **2023**, *2*, 22–39. [CrossRef]
16. Bejan, G.; Bărbuță, M.; Vizitiu, R.Ș.; Burlacu, A. Lightweight Concrete with Waste—Review. *Procedia Manuf.* **2020**, *46*, 136–143. [CrossRef]
17. Samson, G.; Phelipot-Mardelé, A.; Lanos, C. A Review of Thermomechanical Properties of Lightweight Concrete. *Mag. Concr. Res.* **2017**, *69*, 201–216. [CrossRef]
18. Jhatial, A.A.; Goh, W.I.; Mohamad, N.; Rind, T.A.; Sandhu, A.R. Development of Thermal Insulating Lightweight Foamed Concrete Reinforced with Polypropylene Fibres. *Arab. J. Sci. Eng.* **2020**, *45*, 4067–4076. [CrossRef]
19. Jami, T.; Rawtani, D.; Agrawal, Y.K. Hemp Concrete: Carbon-Negative Construction. *Emerg. Mater. Res.* **2016**, *5*, 240–247. [CrossRef]
20. Arehart, J.H.; Nelson, W.S.; Srubar, W.V. On the Theoretical Carbon Storage and Carbon Sequestration Potential of Hempcrete. *J. Clean. Prod.* **2020**, *266*, 121846. [CrossRef]
21. Kumar, V.; Ramadoss, R.; G.S, R. A Study Report on Carbon Sequestration by Using Hempcrete. *Mater. Today Proc.* **2021**, *45*, 6369–6371. [CrossRef]
22. Arehart, J.H.; Hart, J.; Pomponi, F.; D'Amico, B. Carbon Sequestration and Storage in the Built Environment. *Sustain. Prod. Consum.* **2021**, *27*, 1047–1063. [CrossRef]
23. Galván-Ruiz, M.; Hernández, J.; Baños, L.; Noriega-Montes, J.; Rodríguez-García, M.E. Characterization of Calcium Carbonate, Calcium Oxide, and Calcium Hydroxide as Starting Point to the Improvement of Lime for Their Use in Construction. *J. Mater. Civ. Eng.* **2009**, *21*, 694–698. [CrossRef]
24. Yadav, M.; Saini, A. Opportunities & Challenges of Hempcrete as a Building Material for Construction: An Overview. *Mater. Today Proc.* **2022**, *65*, 2021–2028. [CrossRef]
25. Nguyen, T.-T.; Picandet, V.; Amziane, S.; Baley, C. Influence of Compactness and Hemp Hurd Characteristics on the Mechanical Properties of Lime and Hemp Concrete. *Eur. J. Environ. Civ. Eng.* **2009**, *13*, 1039–1050. [CrossRef]

26. Jami, T.; Karade, S.R.; Singh, L.P. A Review of the Properties of Hemp Concrete for Green Building Applications. *J. Clean. Prod.* **2019**, *239*, 117852. [CrossRef]
27. Stevulova, N.; Cigasova, J.; Estokova, A.; Terpakova, E.; Geffert, A.; Kacik, F.; Singovszka, E.; Holub, M. Properties Characterization of Chemically Modified Hemp Hurds. *Materials* **2014**, *7*, 8131–8150. [CrossRef]
28. Bokhari, S.M.Q.; Chi, K.; Catchmark, J.M. Structural and Physico-Chemical Characterization of Industrial Hemp Hurd: Impacts of Chemical Pretreatments and Mechanical Refining. *Ind. Crops Prod.* **2021**, *171*, 113818. [CrossRef]
29. Heinze, T. Cellulose: Structure and Properties. In *Cellulose Chemistry and Properties: Fibers, Nanocelluloses and Advanced Materials*; Rojas, O.J., Ed.; Springer: Cham, Switzerland, 2016; pp. 1–52. ISBN 978-3-319-26015-0.
30. Ebringerová, A.; Hromádková, Z.; Heinze, T. Hemicellulose. In *Polysaccharides I: Structure, Characterization and Use*; Heinze, T., Ed.; Springer: Berlin/Heidelberg, Germany, 2005; pp. 1–67. ISBN 978-3-540-31583-4.
31. Jędrzejczak, P.; Collins, M.N.; Jesionowski, T.; Klapiszewski, Ł. The Role of Lignin and Lignin-Based Materials in Sustainable Construction—A Comprehensive Review. *Int. J. Biol. Macromol.* **2021**, *187*, 624–650. [CrossRef]
32. Van Balen, K.; Van Gemert, D. Modelling Lime Mortar Carbonation. *Mater. Struct.* **1994**, *27*, 393–398. [CrossRef]
33. Shih, S.-M.; Ho, C.-S.; Song, Y.-S.; Lin, J.-P. Kinetics of the Reaction of $Ca(OH)_2$ with CO_2 at Low Temperature. *Ind. Eng. Chem. Res.* **1999**, *38*, 1316–1322. [CrossRef]
34. Liu, M.; Thygesen, A.; Summerscales, J.; Meyer, A.S. Targeted Pre-Treatment of Hemp Bast Fibres for Optimal Performance in Biocomposite Materials: A Review. *Ind. Crops Prod.* **2017**, *108*, 660–683. [CrossRef]
35. Kabir, M.M.; Wang, H.; Lau, K.T.; Cardona, F. Chemical Treatments on Plant-Based Natural Fibre Reinforced Polymer Composites: An Overview. *Compos. Part B Eng.* **2012**, *43*, 2883–2892. [CrossRef]
36. Moonart, U.; Utara, S. Effect of Surface Treatments and Filler Loading on the Properties of Hemp Fiber/Natural Rubber Composites. *Cellulose* **2019**, *26*, 7271–7295. [CrossRef]
37. Prasad, B.M.; Sain, M.M. Mechanical Properties of Thermally Treated Hemp Fibers in Inert Atmosphere for Potential Composite Reinforcement. *Mater. Res. Innov.* **2003**, *7*, 231–238. [CrossRef]
38. Stevulova, N.; Estokova, A.; Cigasova, J.; Schwarzova, I.; Kacik, F.; Geffert, A. Thermal Degradation of Natural and Treated Hemp Hurds under Air and Nitrogen Atmosphere. *J. Therm. Anal. Calorim.* **2017**, *128*, 1649–1660. [CrossRef]
39. Kundu, K.; Chatterjee, A.; Bhattacharyya, T.; Roy, M.; Kaur, A. *Thermochemical Conversion of Biomass to Bioenergy: A Review*; Springer: Berlin/Heidelberg, Germany, 2018; pp. 235–268. ISBN 978-981-10-7517-9.
40. Collet, F.; Pretot, S. Thermal Conductivity of Hemp Concretes: Variation with Formulation, Density and Water Content. *Constr. Build. Mater.* **2014**, *65*, 612–619. [CrossRef]
41. Nguyen, T.T.; Picandet, V.; Carre, P.; Lecompte, T.; Amziane, S.; Baley, C. Effect of Compaction on Mechanical and Thermal Properties of Hemp Concrete. *Eur. J. Environ. Civ. Eng.* **2010**, *14*, 545–560. [CrossRef]
42. Abdellatef, Y.; Khan, M.A.; Khan, A.; Alam, M.I.; Kavgic, M. Mechanical, Thermal, and Moisture Buffering Properties of Novel Insulating Hemp-Lime Composite Building Materials. *Materials* **2020**, *13*, 5000. [CrossRef]
43. Isaac, R.A. *AOAC: Official Methods of Analysis (Volume 1)*; Association of Official Analytical Chemists, Inc.: Washington, DC, USA, 1990; Chapter 3, pp. 40–63.
44. *ASTM C127-15*; Standard Test Method for Relative Density (Specific Gravity) and Absoprtion of Coarse Aggregate. ASTM International: West Conshohocken, PA, USA, 2024.
45. *ASTM C128-22*; Standard Test Method for Relative Density (Specific Gravity) and Absorption of Fine Aggregate. ASTM International: West Conshohocken, PA, USA, 2023.
46. *ASTM C642-21*; Standard Test Method for Density, Absorption, and Voids in Hardened Concrete. ASTM International: West Conshohocken, PA, USA, 2009.
47. *ASTM D5334-08*; Standard Test Method for Determination of Thermal Conductivity of Soil and Soft Rock by Thermal Needle Probe Procedure. ASTM International, American Society for Testing and Materials: West Conshohocken, PA, USA, 2014.
48. D'Eusanio, V.; Malferrari, D.; Marchetti, A.; Roncaglia, F.; Tassi, L. Waste By-Product of Grape Seed Oil Production: Chemical Characterization for Use as a Food and Feed Supplement. *Life* **2023**, *13*, 326. [CrossRef]
49. D'Eusanio, V.; Lezza, A.; Anderlini, B.; Malferrari, D.; Romagnoli, M.; Roncaglia, F. Technological Prospects of Biochar Derived from Viticulture Waste: Characterization and Application Perspectives. *Energies* **2024**, *17*, 3421. [CrossRef]
50. Johnson, C.M. Differential Scanning Calorimetry as a Tool for Protein Folding and Stability. *Arch. Biochem. Biophys.* **2013**, *531*, 100–109. [CrossRef]
51. Ojeda-Galván, H.J.; Hernández-Arteaga, A.C.; Rodríguez-Aranda, M.C.; Toro-Vazquez, J.F.; Cruz-González, N.; Ortíz-Chávez, S.; Comas-García, M.; Rodríguez, A.G.; Navarro-Contreras, H.R. Application of Raman Spectroscopy for the Determination of Proteins Denaturation and Amino Acids Decomposition Temperature. *Spectrochim. Acta A Mol. Biomol. Spectrosc.* **2023**, *285*, 121941. [CrossRef]
52. Şen, D.; Gökmen, V. Kinetic Modeling of Maillard and Caramelization Reactions in Sucrose-Rich and Low Moisture Foods Applied for Roasted Nuts and Seeds. *Food Chem.* **2022**, *395*, 133583. [CrossRef]
53. Weiss, I.M.; Muth, C.; Drumm, R.; Kirchner, H.O.K. Thermal Decomposition of the Amino Acids Glycine, Cysteine, Aspartic Acid, Asparagine, Glutamic Acid, Glutamine, Arginine and Histidine. *BMC Biophys.* **2018**, *11*, 2. [CrossRef]
54. Salema, A.A.; Ting, R.M.W.; Shang, Y.K. Pyrolysis of Blend (Oil Palm Biomass and Sawdust) Biomass Using TG-MS. *Bioresour. Technol.* **2019**, *274*, 439–446. [CrossRef]

55. Wang, S.; Dai, G.; Yang, H.; Luo, Z. Lignocellulosic Biomass Pyrolysis Mechanism: A State-of-the-Art Review. *Prog. Energy Combust. Sci.* **2017**, *62*, 33–86. [CrossRef]
56. Ding, Y.; Huang, B.; Li, K.; Du, W.; Lu, K.; Zhang, Y. Thermal Interaction Analysis of Isolated Hemicellulose and Cellulose by Kinetic Parameters during Biomass Pyrolysis. *Energy* **2020**, *195*, 117010. [CrossRef]
57. Carrier, M.; Loppinet-Serani, A.; Denux, D.; Lasnier, J.-M.; Ham-Pichavant, F.; Cansell, F.; Aymonier, C. Thermogravimetric Analysis as a New Method to Determine the Lignocellulosic Composition of Biomass. *Biomass Bioenergy* **2011**, *35*, 298–307. [CrossRef]
58. Yang, H.; Yan, R.; Chin, T.; Liang, D.T.; Chen, H.; Zheng, C. Thermogravimetric Analysis−Fourier Transform Infrared Analysis of Palm Oil Waste Pyrolysis. *Energy Fuels* **2004**, *18*, 1814–1821. [CrossRef]
59. Hosoya, T.; Kawamoto, H.; Saka, S. Cellulose–Hemicellulose and Cellulose–Lignin Interactions in Wood Pyrolysis at Gasification Temperature. *J. Anal. Appl. Pyrolysis* **2007**, *80*, 118–125. [CrossRef]
60. Zhao, C.; Jiang, E.; Chen, A. Volatile Production from Pyrolysis of Cellulose, Hemicellulose and Lignin. *J. Energy Inst.* **2017**, *90*, 902–913. [CrossRef]
61. Yeo, J.Y.; Chin, B.L.F.; Tan, J.K.; Loh, Y.S. Comparative Studies on the Pyrolysis of Cellulose, Hemicellulose, and Lignin Based on Combined Kinetics. *J. Energy Inst.* **2019**, *92*, 27–37. [CrossRef]